Supplementary Information for ‘Simulating the Earth system response to negative emissions.’

C D Jones[1], P Ciais[2], S J Davis[3], P Friedlingstein[4], T Gasser[5,2], G P Peters[6], J Rogelj[7,8], D P van Vuuren[9,10], J G Canadell[11], A Cowie[12], R B Jackson[13], M Jonas[14], E Kriegler[15], E Littleton[16], J A Lowe[1], J Milne[17], G Shrestha[18], P Smith[19], A Torvanger[20] and A Wiltshire[1]

Methods: use of CMIP5 ESMs and processing of concentration-driven scenario simulations.

Section 2 of the main text analyses results from CMIP5 Earth system model simulations. Although we can only draw on 4 models here they span a reasonable spread in the bigger multi-model ensemble which is available up to 2100. The models span global temperature rise at 2100 from 1.8 to 2.4 K above pre-industrial and 2080-2100 global emissions from -1.1 to +1.4 GtC yr^{-1}.

Table S1 shows the observed and RC2.6 scenario values for anthropogenic emissions broken down into gross positive (fossil fuel and land-use change emissions) and gross negative (NETs) terms, and changes in atmospheric CO_2 expressed in units of ppm as commonly reported and also converted into GtC for direct comparison with other rows in the table. Also shown are the model results from the four CMIP5 ESMs and from the MAGICC model, which is the simple climate model used to convert IAM emissions into atmospheric CO_2 concentrations (Meinshausen et al., 2011).

CMIP5 experimental design includes coupled climate-carbon cycle simulations which are both concentration-driven and emissions-driven (see e.g. Box 6.4 of Ciais et al., 2013). However, only concentration-driven simulations were extended past 2100 with multiple ESMs, and so our analysis draws on those results. In these numerical experiments the CO_2 concentration pathway is prescribed as a boundary condition for the models which then simulate the land and ocean carbon fluxes. From these we diagnose the compatible anthropogenic emissions as the emission that would have been required to drive the changes in CO_2 given the simulated land and ocean fluxes. This allows us to compare simulations for the same CO_2 concentration pathway across multiple models and infer how the Earth system responds over time to changes in the rates of emissions and sinks.

Figure 3(a) in the main text shows the prescribed atmospheric CO_2 concentration from the RCP2.6 scenario which is used as input to all the ESMs. Panels (b)-(d) then show the land and ocean fluxes which are simulated by the models in response to this prescribed concentration scenario.

Figure 4 in the main text uses the waterfall format of figure 1 to depict the changes in time of the different components of the global carbon budget under the RCP2.6 extension to 2300. To construct this figure, we took data from different sources as follows. In each panel:

- The first bar in each panel shows the atmospheric CO_2 concentration at the start of the 50-year period. In the case of panel (a) this is the observed concentration for the year 2000, and for the other panels it is taken from the RCP2.6 scenario.
- To this we add the anthropogenic emissions from the scenario averaged over the 50-year period. These are shown by the second and third bar in each panel and represent the split between positive emissions due to fossil fuel and land-use change, and negative emissions due to NETs.
- The next two bars show the simulated land and ocean carbon uptake averaged over the 50-year period and averaged across all four ESMs. In the figure we just show the model mean, but the full model range can be seen in figure 3, panels (c) and (d). Table S1 lists the mean and standard deviation across models for each 50-year period.
- The final bar shows the atmospheric CO_2 concentration that would result from this balance of fluxes at the end of the 50-year period. Because we have mixed the emissions from the IMAGE integrated assessment model with the sinks from the CMIP5 ESMs the calculated change in CO_2 does not match precisely the CO_2 pathway prescribed from the scenario. For example, panel (a) shows a CO_2 concentration for 2050 of 450ppm, whereas panel (b) shows the scenario value for 2050 of 443 ppm. This difference is because the CO_2 in the scenario was derived using the MAGICC model. Figure 3(b) shows that the land and ocean combined sink simulated by MAGICC is close to, but not identical to, the ESM mean.

Table S1. CO_2 concentration and simulated response of land and ocean sinks for the RCP2.6 and the 4 CMIP5 ESMs. All values are averages over each 50 year period, expressed as mean fluxes or rates of change in GtC per year (except the penultimate row which is ppm per year). First 3 rows, labeled as "Anthropogenic" are from the RCP2.6 scenario. The CMIP5 entries are the mean and standard deviation over the 4 models listed in table 1of the main text. The MAGICC natural flux is inferred as the difference between the RCP2.6 scenario emissions and CO_2 concentration.

		Historical period			RCP2.6					
Source		1850-1900	1900-1950	1950-2000	2000-2050	2050-2100	2100-2150	2150-2200	2200-2250	2250-2300
Observed / scenario	Anthropogenic fossil and land-use emission / GtC yr^{-1}	0.88	1.88	5.67	7.98	3.53	2.69	2.69	2.69	2.69
	Anthropogenic NET / GtC yr^{-1}	0	0	0	-0.58	-2.61	-3.11	-3.11	-3.11	-3.11
	Anthropogenic total / GtC yr^{-1}	0.88	1.88	5.67	7.4	0.92	-0.42	-0.42	-0.42	-0.42
Observed / scenario	Change in atmospheric CO_2 / ppm yr^{-1}	0.24	0.30	1.16	1.48	-0.44	-0.43	-0.31	-0.24	-0.22
	Change in atmospheric CO_2 / GtC yr^{-1}	0.51	0.64	2.46	3.14	-0.93	-0.91	-0.66	-0.51	-0.47
CMIP5 ESMs	Land flux / GtC yr^{-1}	0.08 ± 0.21	0.18 ± 0.14	-0.38 ± 0.16	-1.66 ± 1.22	-0.83 ± 0.91	-0.43 ± 1.41	-0.06 ± 0.80	0.22 ± 0.56	0.36 ± 0.39
	ocean flux / GtC yr^{-1}	-0.31 ± 0.15	-0.60 ± 0.21	-1.37 ± 0.22	-2.32 ± 0.35	-1.13 ± 0.34	-0.54 ± 0.30	-0.32 ± 0.24	-0.23 ± 0.22	-0.10 ± 0.20
	natural (land plus ocean) total flux / GtC yr^{-1}	-0.23 ± 0.20	-0.42 ± 0.12	-1.75 ± 0.30	-3.97 ± 1.52	-1.96 ± 1.10	-0.98 ± 1.40	-0.38 ± 0.76	-0.01 ± 0.45	0.27 ± 0.27
MAGICC	MAGICC natural (land plus ocean) total flux / GtC yr^{-1}	-0.32	-1.21	-3.20	-4.60	-1.69	-0.50	-0.24	-0.10	-0.04

Documenting the simple climate-carbon cycle model

To explore the scenario dependence of the cumulative airborne fraction (CAF) of negative emissions we use a simple climate-carbon cycle model that has been documented and used elsewhere (e.g. Jones et al., 2003; 2006; House et al., 2008; Huntingford et al., 2009).

Jones et al. (2003) and Jones et al. (2006) describe the model in detail. Briefly, it comprises a global box model of climate and the carbon cycle. For the land carbon cycle GPP is simulated as a Michaelis-Menton function of CO_2 and a quadratic function of temperature. GPP leads to an increase in vegetation carbon which turnover to form soil carbon which itself respires to the atmosphere. The ocean carbon cycle is represented by an impulse response function after Joos et al., (1996).

Simple model parameters used for this study are very close to those used in Jones et al. (2003), and close to the most likely of the frequency distributions shown in figure 4 of Jones et al. (2006). We adopt here: q10 =2 for both soil and plant respiration, CI_half=350 which corresponds to CA_half of 437.50 ppm (based on a ratio of internal to atmospheric CO_2 of CI:CA=0.8). d2GPP/dT2 = -0.006 K^{-2} and dGPP/dT=0 which leads to a T_{opt}=0. In this configuration it closely mimics the HadCM3LC model.

The model was first tested for the four RCP scenarios in concentration driven mode using CO_2 forcing data used in CMIP5. From these simulations we can infer the compatible emissions that would be required to follow the prescribed CO_2 pathway. Figure S1 shows the emissions diagnosed from these simulations compared with the emissions from the RCPs. Agreement is very close.

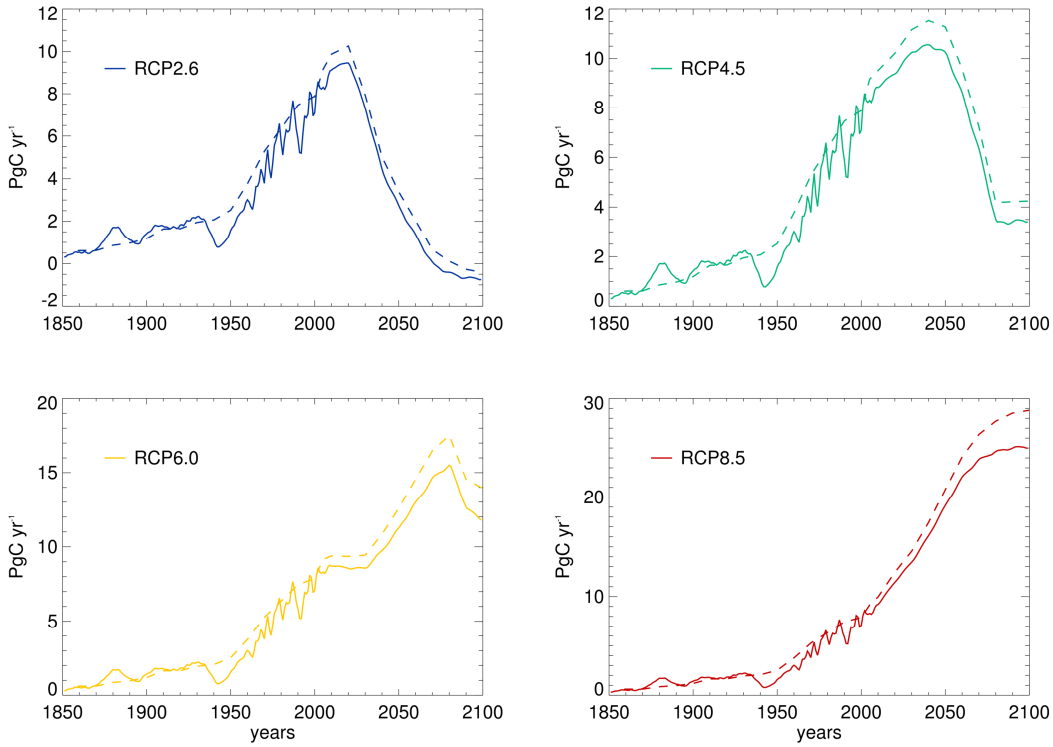

Figure S1. Compatible CO_2 emissions diagnosed from concentration-driven simple model simulations (solid lines) compared with those from the RCPs (dashed lines). RCP2.6 (top left), RCP4.5 (top right), RCP6.0 (lower left), RCP8.5 (lower right).

A second test is to perform these simulations in emissions-driven mode, forcing the model with the RCP CO_2 emissions and simulating the atmospheric concentration. Figure S2 shows close agreement, although the simple model projects slightly too high CO_2 compared with the RCP pathway for all four scenarios.

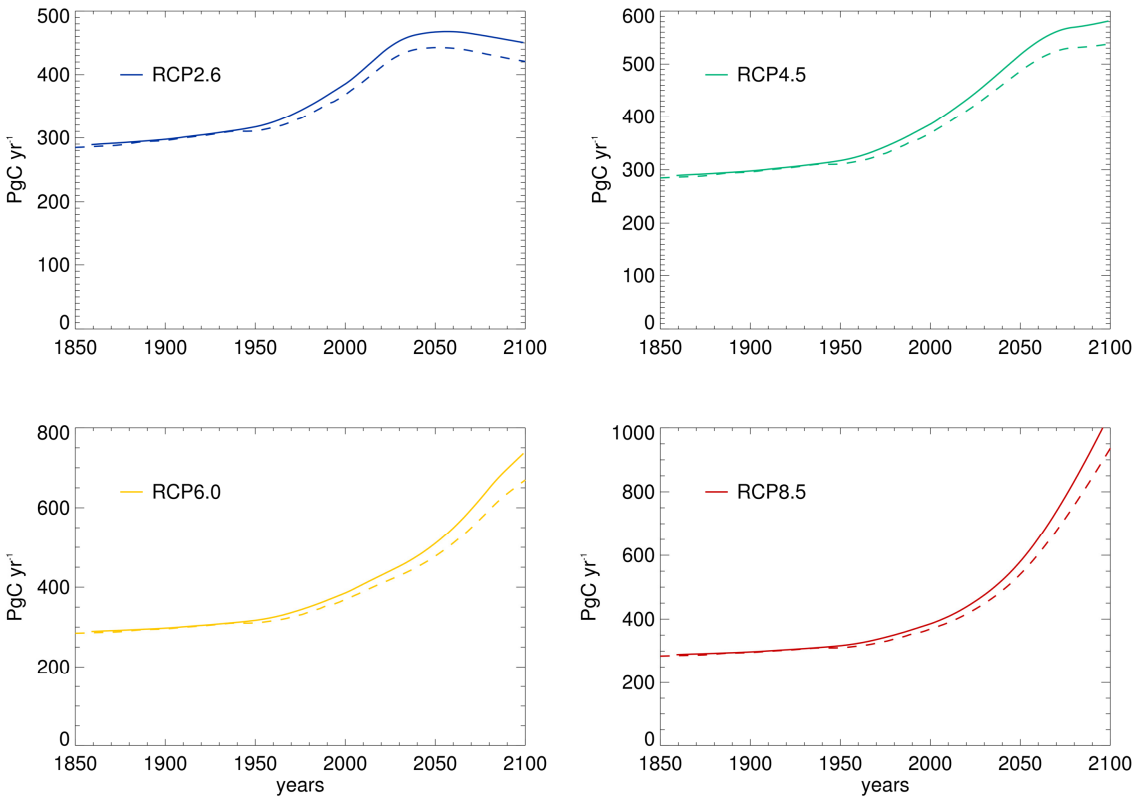

Figure S2. Atmospheric CO_2 concentration simulated in emission-driven simple model simulations (solid lines) compared with those from the RCPs (dashed lines). RCP2.6 (top left), RCP4.5 (top right), RCP6.0 (lower left), RCP8.5 (lower right).

Deriving cumulative airborne fraction metrics

Section 3 of the main text describes results from some cumulative airborne fraction metrics used to quantify the impact on the Earth system of the additional NETs applied to the RCP scenarios. Figure S3 shows the scenario of emissions applied and the derivation of the cumulative airborne fraction metrics. Each row of the figure shows the same quantity, but arranged from left to right for each scenario: RCP2.6 (blue lines); RCP4.5 (green); RCP6.0 (yellow); RCP8.5 (red).

The top row (panels a-d) shows the cumulative emissions from 2020 with the un-modified RCP scenario in solid lines, and the scenarios with additional NETs in dashed lines. The values by 2100 are shown in table 2 of the main text, in columns 3 and 5.

The second row (panels e-h) shows the cumulative airborne fraction (CAF) of the simulations. This is defined as the change in atmospheric CO_2 since 2020 in each simulation divided by the cumulative emission since 2020. Un-modified RCP scenarios are shown by solid lines, and the scenarios with additional NETs in dashed lines. The values by 2100 are shown in table 2 of the main text, in columns 7 and 8. As described in the main text it is particularly the case for RCP2.6 that this measure varies markedly and can change rapidly in both magnitude and sign especially if the cumulative emissions change sign. In this case the simulation with a constant 4 GtC yr^{-1} of NETs achieves negative cumulative emission at 2080 and this drives a singularity in the cumulative airborne fraction defined here.

The third row (panels i-l) shows the reduction in atmospheric CO_2 between the 4 modified (additional NETs) simulations and the un-modified RCP simulation. Although the form of these results appears similar for all RCPs, the magnitude differs.

The fourth row (panels m-p) shows the cumulative airborne fraction *of* the NETs. This is defined as the difference in CO_2 between the two simulations (with and without the additional NETs) divided by the cumulative emissions to that year. This is referred to in the main text as the "perturbation airborne fraction" (PAF) and the values by 2100 are shown in table 2 of the main text, in column 9. This quantity differs from that of the second row because it is calculated from the change in CO_2 concentration for the same year between simulations rather than the change in CO_2 between years in a single simulation.

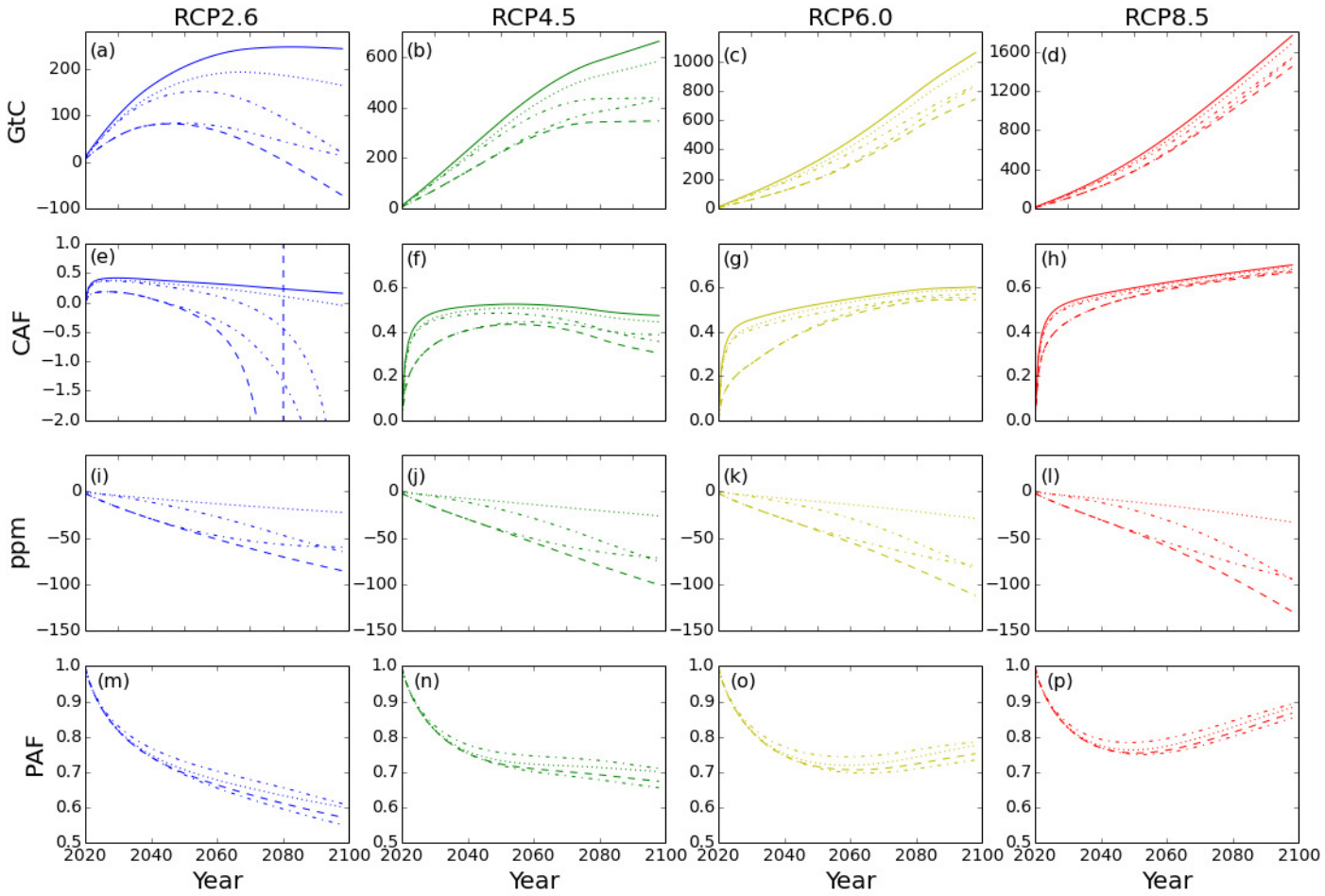

Figure S3.Cumulative emissions and airborne fraction metrics from RCP simulations with additional NETs. (a-d) cumulative emissions since 2020; (e-h) cumulative airborne fraction; (i-l) resulting change in atmospheric CO_2 concentration; (m-p) perturbation airborne fraction. See SI text for full details.

References

Ciais, P, et al. 2013 Carbon and Other Biogeochemical Cycles. In: Climate Change 2013: The Physical Science Basis. Contribution of Working Group I to the Fifth Assessment Report of the Intergovernmental Panel on Climate Change [Stocker, T.F., D. Qin, G.-K. Plattner, M. Tignor, S.K. Allen, J. Boschung, A. Nauels, Y. Xia, V. Bex and P.M. Midgley (eds.)]. Cambridge University Press, Cambridge, United Kingdom and New York, NY, USA.

House J, Huntingford C, Knorr W, Cornell S E, Cox P M, Harris G R, Jones C D, Lowe J A and Prentice C I 2008 What do recent advances in quantifying climate and carbon cycle uncertainties mean for climate policy? *Environ. Res. Lett*. 3044002

Huntingford, C, Lowe, J A, Booth, B B B, Jones, C D, Harris, G R, Gohar L K and Meir P 2009 Contributions of carbon cycle uncertainty to future climate projection spread. *Tellus*, **61B**, 355-360

Jones, C D, Cox, P M and Huntingford, C 2003 Uncertainty in climate-carbon cycle projections associated with the sensitivity of soil respiration to temperature. *Tellus* **55B**, 642–648.

Jones, C D, Cox, P M and Huntingford, C 2006 Climate-carbon cycle feedbacks under stabilization: uncertainty and observational constraints. *Tellus*, **58B**, 603-613

Joos, F, Bruno, M, Fink, R, Siegenthaler, U, Stocker, T, Le Quéré, C and Sarmiento, J 1996 An efficient and accurate representation of complex oceanic and biospheric models of anthropogenic carbon uptake. *Tellus,* **48B**, 397–417

Meinshausen, M, et al. 2011 The RCP Greenhouse Gas Concentrations and their Extension from 1765 to 2300, *Clim. Change*, Special RCP Issue.